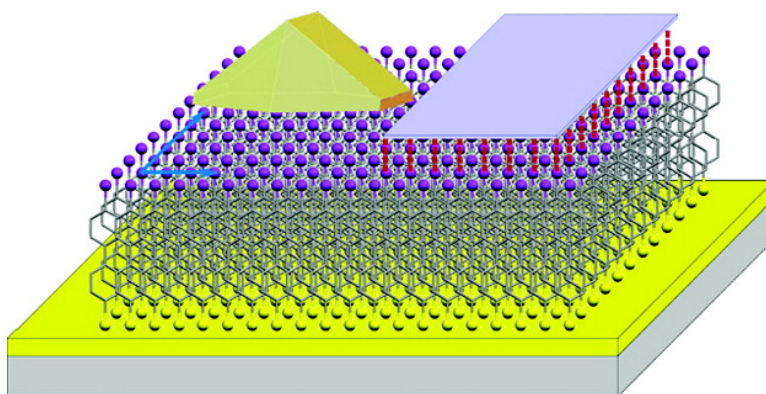**Article**

Controlling Molecular Crystal Polymorphism with Self-Assembled Monolayer Templates

Rupa Hiremath, Joseph A. Basile, Stephen W. Varney, and Jennifer A. Swift

More About This Article

Additional resources and features associated with this article are available within the HTML version:

- Supporting Information
- Links to the 17 articles that cite this article, as of the time of this article download
- Access to high resolution figures
- Links to articles and content related to this article
- Copyright permission to reproduce figures and/or text from this article

View the Full Text HTML

Controlling Molecular Crystal Polymorphism with Self-Assembled Monolayer Templates

Rupa Hiremath, Joseph A. Basile, Stephen W. Varney, and Jennifer A. Swift*

Contribution from the Department of Chemistry, Georgetown University, 37th and "O" Streets NW, Washington, D.C. 20057-1227

Received September 27, 2005; E-mail: jas2@georgetown.edu

Abstract: The control of crystal polymorphism is a long-standing issue in solid-state chemistry, which has many practical implications for a variety of commercial applications. At least four different crystalline forms of 1,3-bis(*m*-nitrophenyl) urea (MNPU), a classic molecular crystal system, are known to crystallize from solution in various concomitant combinations. Herein we demonstrate that the introduction of gold−thiol self-assembled monolayers (SAMs) of substituted 4′-X-mercaptobiphenyls (X = H, I, and Br) into the crystallization solution can serve as an effective means to selectively template the nucleation and growth of α-, β-, and γ-MNPU phases, respectively. Polymorph control in the presence of SAM surfaces persists under a variety of solution conditions and consistently results in crystalline materials with high phase purity. The observed selectivity is rationalized on the basis of long-range two-dimensional geometric lattice matching and local complementary chemical interactions at the SAM/crystal interfaces.

Introduction

One of the long-standing challenges in organic solid-state chemistry is the ability to predict and control the occurrence of polymorphism, the ability of a molecule to crystallize in more than one packing arrangement.[1] This has broad practical implications for a number of industries, ranging from pharmaceuticals (drugs) to textiles (dyes and pigments) to defense (energetic materials). While in principle it may be possible to experimentally define the occurrence domain(s)[2] under which a particular form of a molecular solid crystallizes, establishing such conditions in practice can be far more complicated than simply specifying a narrow range of solvents, temperatures, and cooling/evaporation rates. There are also a number of examples in which two or more polymorphs form concomitantly under essentially the same crystallization conditions.[3] In part, this may be a consequence of the fact that crystallization begins with the nucleation stage, usually considered to be a heterogeneous process, and the total contents of any given solution can never be completely known.

While the conventional methods of polymorph screening by slurry conversion and/or varying solvent, temperature, and supersaturation have been very much accelerated by the use of high throughput screening methods,[4,5] a variety of complementary approaches to controlling and/or discovering new polymorphs have also been pursued in recent years. These include crystallization in confined spaces, such as capillaries[6,7] and micropores,[8] or in the presence of molecular[9,10] or polymeric[11−13] additives. Polymorph control has also been achieved by epitaxial nucleation and growth on single-crystal substrates.[14,15]

Other types of ordered 2D surfaces, such as Langmuir films and self-assembled monolayers (SAMs), have been used to selectively nucleate and grow a number of different inorganic crystals,[16−22] though their use as templates for molecular crystals has been somewhat more limited.[23−27] In such studies, the templating function is generally attributed to strong ionic or hydrogen-bonding interactions formed across the monolayer/crystal interface. In our own recent work, we have shown that

(1) Bernstein, J. *Polymorphism in Molecular Crystals*; Oxford University Press: New York, 2002.
(2) Sato, K.; Boistelle, R. *J. Cryst. Growth* **1984**, *66*, 441−450.
(3) Bernstein, J.; Davey, R. J.; Henck, J.-O. *Angew. Chem., Int. Ed.* **1999**, *38*, 3440−3461.
(4) Peterson, M. L.; Morissette, S. L.; McNulty, C.; Goldsweig, A.; Shaw, P.; LeQuesne, M.; Monagle, J.; Encina, N.; Marchionna, J.; Johnson, A.; Cima, M. J.; Almarsson, O. *J. Am. Chem. Soc.* **2002**, *124*, 10858−10959.
(5) Morissette, S. L.; Soukasene, S.; Levinson, D. A.; Cima, M., J.; Almarsson, O. *Proc. Natl. Acad. Sci. U.S.A.* **2003**, *100*, 2180−2184.
(6) Chyall, L. J.; Tower, J. M.; Coates, D. A.; Houston, T. L.; Childs, S. L. *Cryst. Growth Des.* **2002**, *2*, 505−510.
(7) Hilden, J. L.; Reyes, C. E.; Kelm, M. J.; Tan, J. S.; Stowell, J. G.; Morris, K. R. *Cryst. Growth Des.* **2003**, *3*, 921−926.
(8) Ha, J.-M.; Wolf, J. H.; Hillmyer, M. A.; Ward, M. D. *J. Am. Chem. Soc.* **2004**, *126*, 3382−3383.
(9) Weissbuch, I.; Popovitz-Biro, R.; Lahav, M.; Leiserowitz, L. *Acta Crystallogr.* **1995**, *B51*, 115−148.
(10) Davey, R. J.; Blagden, N.; Potts, G. D.; Docherty, R. *J. Am. Chem. Soc.* **1997**, *119*, 1767−1772.
(11) Staab, E.; Addadi, L.; Leiserowitz, L.; Lahav, M. *Adv. Mater.* **1990**, *2*, 40−43.
(12) Lang, M.; Grzesiak, A. L.; Matzger, A. J. *J. Am. Chem. Soc.* **2002**, *124*, 14834−14835.
(13) Price, C. P.; Grzesiak, A. L.; Matzger, A. J. *J. Am. Chem. Soc.* **2005**, *127*, 5512−5517.
(14) Bonafede, S. J.; Ward, M. D. *J. Am. Chem. Soc.* **1995**, *117*, 7853−7861.
(15) Mitchell, C. A.; Yu, L.; Ward, M. D. *J. Am. Chem. Soc.* **2001**, *123*, 10830−10839.
(16) Heywood, B. R.; Mann, S. *Adv. Mater.* **1994**, *16*, 9−20.
(17) Popovitz-Biro, R.; Lahav, M.; Leiserowitz, L. *J. Am. Chem. Soc.* **1991**, *113*, 8943−8944.
(18) Aizenberg, J.; Black, A. J.; Whitesides, G. M. *J. Am. Chem. Soc.* **1999**, *121*, 4500−4509.
(19) Kuther, J.; Seshadri, R.; Knoll, W.; Tremel, W. *J. Mater. Chem.* **1998**, *8*, 641−650.
(20) Travaille, A. M.; Kaptjin, L.; Verwer, P.; Hulsken, B.; Elemans, J. A. A. W.; Nolte, R. J. M.; van Kempen, H. *J. Am. Chem. Soc.* **2003**, *125*, 11571−11577.
(21) Bandyopadhyay, K.; Vijayamohanan, K. *Langmuir* **1998**, *14*, 6924−6929.
(22) Meldrum, F. C.; Flath, J.; Knoll, W. *Langmuir* **1997**, *13*, 2033−2049.
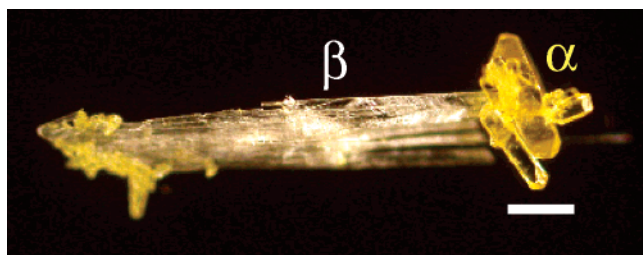
Figure 1. Yellow prisms of the α form and white needles of the β form grow concomitantly from supersaturated ethanol solutions. Scale bar = 1 mm.

SAM templates can be used to control the absolute growth direction of polar crystals of 4-iodo-4′-nitrobiphenyl[28] and to selectively nucleate a less stable form 2-iodo-4-nitroaniline.[29] These studies also demonstrate that weaker forces at the SAM/crystal interface, such as I···NO$_2$ and van der Waals interactions, can be used to direct the nucleation process.

In the present study, we apply SAM template methods to the problem of controlling polymorphism in a classic molecular crystal system, 1,3-bis(*m*-nitrophenyl) urea (MNPU). First studied in the late 19th century,[30−32] MNPU was identified by Groth as having at least three different phases—α, β, and γ.

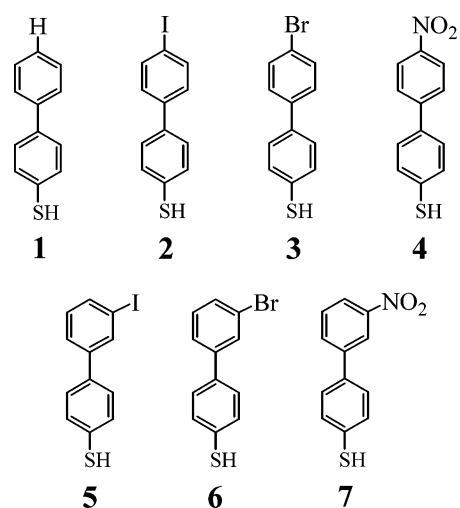1,3-bis(*m*-nitrophenyl) urea (MNPU)
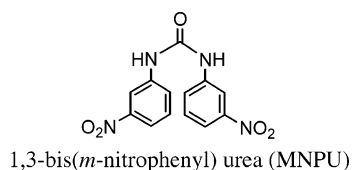
The α (yellow prisms), β (white needles), and γ (yellow plates) phases are visually distinguishable, but often crystallize concomitantly from aqueous ethanol solutions (Figure 1). Nearly a century later, Etter et al.[33−35] reported the first crystal structures for the α (*P2$_1$/c*: $a = 11.495$ Å, $b = 13.816$ Å, $c = 8.307$ Å, $\beta = 91.92°$) and β (*C2*: $a = 20.95$ Å, $b = 7.412$ Å, $c = 6.715$ Å, $\beta = 104.96°$) forms as part of a larger study on the hydrogen-bonding patterns and cocrystallization behavior of diaryl ureas. At the time our SAM template study was initiated, the structure of the γ form was unknown. In the course of our work, we were able to determine that the γ phase is actually a monohydrate (*C2*: $a = 24.876$ Å, $b = 7.386$ Å, $c = 3.757$ Å, $\beta = 96.85°$). Bernstein et al.[36] also recently obtained the crystal

structure of the γ monohydrate phase and, serendipitously, discovered a previously unknown anhydrous phase, δ, (*P2$_1$/c*: $a = 4.686$ Å, $b = 18.427$ Å, $c = 17.72$ Å, $\beta = 90.5°$) which crystallizes as white needles. Depending on the solution conditions, they observed that the known crystal phases grew concomitantly in various combinations, but despite attempts to identify the individual occurrence domains for each of the four phases, only the β form could be consistently obtained with high phase purity using conventional crystallization methods.[36]

In the present work, we demonstrate that three of the MNPU phases—α, β and γ—can each be selectively nucleated and reproducibly grown on appropriately functionalized mercapto-biphenyl SAM templates. The control over nucleation is rationalized on the basis of favorable intermolecular and geometric interactions at the SAM/crystal interface.

Experimental Section

Synthesis. 1,3-Bis(*m*-nitrophenyl) Urea (MNPU) was synthesized according to the literature[34] by stirring 1:1 mixtures of 3-nitrophenyl isocyanate (Aldrich, 97%) and 3-nitroaniline (Aldrich, 98%) in benzene for 24 h at room temperature under dry nitrogen. The product readily precipitates and is easily isolated in pure form (mp = 256−258 °C, in agreement with previous reports).

4′-Bromo-4-mercaptobiphenyl (3) was prepared according to the literature.[37] Tetrakis(triphenylphosphine) palladium catalyst (0.2 mmol, Aldrich, 99%) was added (under dry N$_2$) to a solution of 1-bromo-4-iodobenzene (20 mmol, Alfa Aesar, 97%+) in 10 mL of anhydrous THF and brought to gentle reflux with stirring. A Grignard solution was prepared from mixing 4-bromothioanisole (20 mmol, Aldrich, 97%) and magnesium turnings (20 mmol, Aldrich, 98%) in 25 mL of anhydrous tetrahydrofuran (Aldrich, 99.9%) over 70 min. The Grignard solution was transferred dropwise to the boiling 1-bromo-4-iodobenzene solution. After addition was completed, the mixture was held under reflux for an additional 30 min. After cooling to room temperature, the mixture was poured into an ice-cold solution of 5% HCl. The resulting solid intermediate, 4′-bromo-4-methylthiobiphenyl, was vacuum filtered, washed with distilled water, dried on the aspirator, and recrystallized from 1:1

(23) Frostman, L. M.; Bader, M. M.; Ward, M. D. *Langmuir* **1994**, *10*, 576−582.
(24) Kang, J. F.; Zaccaro, J.; Ulman, A.; Myerson, A. *Langmuir* **2000**, *16*, 3791−3796.
(25) Lee, A. Y.; Ulman, A.; Myerson, A. S. *Langmuir* **2002**, *18*, 5886−5898.
(26) Banno, N.; Nakanishi, T.; Matsunaga, M.; Asahi, T.; Osaka, T. *J. Am. Chem. Soc.* **2004**, *126*, 428−429.
(27) Briseno, A. L.; Aizenberg, J.; Han, Y.-J.; Penkala, R. A.; Moon, H.; Lovinger, A. J.; Kloc, C.; Bao, Z. *J. Am. Chem. Soc.* **2005**, *127*, 12164−12165.
(28) Hiremath, R.; Varney, S. W.; Swift, J. A. *Chem. Mater.* **2004**, *16*, 4948−4954.
(29) Hiremath, R.; Varney, S. W.; Swift, J. A. *Chem. Commun.* **2004**, 2676−2677.
(30) Offret, A.; Vittenet, H. *Bull. Soc. Chim. Fr.* **1899**, *21*, 151−153.
(31) Offret, A.; Vittenet, H. *Bull. Soc. Chim. Fr.* **1899**, *22*, 788−797.
(32) Groth, P. *An Introduction to Chemical Crystallography*; Wiley: New York, 1906.
(33) Etter, M.; Panuto, T. *J. Am. Chem. Soc.* **1988**, *110*, 5896−5897.
(34) Etter, M. C.; Urbanczyk-Lipkowska, Z.; Zia-Ebrahimi, M.; Pannuto, T. W. *J. Am. Chem. Soc.* **1990**, *112*, 8415−8426.
(35) Huang, K.-S.; Britton, D.; Etter, M. C.; Byrn, S. R. *J. Mater. Chem.* **1995**, *5*, 379−383.
(36) Rafilovich, M.; Bernstein, J.; Harris, R. K.; Apperley, D. C.; Karamertzanis, P. G.; Price, S. L. *Cryst. Growth Des.* **2005**, *5*(6), 2197−2209.

(37) Ulman, A. *Acc. Chem. Res.* **2001**, *34*, 855−863.

heptane:2-propanol: mp 150−151 °C; ¹H NMR (δ ppm, CDCl₃) 2.52 (3H), 7.30−7.34 (4H), 7.41−7.56 (4H).

4′-Bromo-4-methylthiobiphenyl (4 mmol) was subsequently reduced by dissolving it in 12 mL of anhydrous *N,N*-dimethylformamide (Aldrich, 99.8%) under dry nitrogen and adding 4 mmol of sodium ethanethiolate (Aldrich, 80%). It was stirred and refluxed gently for 6 h. After cooling to room temperature, the mixture was poured into a solution of ice-cold 5% HCl. The solid was vacuum filtered, washed with distilled water, and dried on the aspirator. The solid was recrystallized in 1:1 heptane:2-propanol and purified by silica gel column chromatography (1:1 CH₂Cl₂:hexane): mp 152−154 °C; ¹H NMR (δ ppm, CDCl₃) 2.52 (1H), 7.30−7.39 (4H), 7.48−7.51 (4H).

3′-Bromo-4-mercaptobiphenyl (6) was prepared according to the literature as for **3**, substituting 1-bromo-3-iodobenzene (Aldrich, 98%) for 1-bromo-4-iodobenzene. Data for the 3′-bromo-4-methylthiobiphenyl intermediate: mp 123−124 °C; ¹H NMR (δ ppm, CDCl₃) 2.52 (3H), 7.25−7.33 (4H), 7.48−7.51 (4H). Data for (**6**): mp 187−188 °C; ¹H NMR (δ ppm, CDCl₃) 2.52 (1H), 7.29−7.34 (4H), 7.79−7.51 (4H).

4-Mercaptobiphenyl (**1**), 4′-iodo-4-mercaptobiphenyl (**2**), 4′-nitro-4-mercaptobiphenyl (**4**), 3′-iodo-4-mercaptobiphenyl (**5**), and 3′-nitro-4-mercaptobiphenyl (**7**) were prepared under analogous reaction conditions. Their syntheses and characterization have been reported elsewhere.[28,29]

All solvents were obtained from Aldrich, EM Science (ACS grade), and Fischer Scientific (HPLC grade) and used without further purification. All melting points reported were determined by Differential Scanning Calorimetry (Thermal Instruments, Richmond, VA) at a heating rate of 5°/min. ¹H NMR spectra were measured using a Mercury 300 MHz (Varian) NMR spectrometer in CDCl₃ solution at ambient temperature. All chemical shifts (δ) are referenced to tetramethylsilane (TMS). Comparison of the experimental and literature values confirms the identities of the products.

Monolayer Preparation and Characterization. Gold substrates (3000 Å, 5 mm²) were prepared in the Georgetown Advanced Electronics Laboratory (GAEL) via high-pressure gold sputtering. Mica squares (5 mm²) were placed on glass slides using Post-it adhesive and double-sided tape. Scotch tape was used to remove the top layer, revealing a fresh layer for exposure to sputtering. A 30 Å layer of chromium was deposited at a rate of 3 Å/s, followed by 3000 Å of gold. The average mean roughness (R_a)[38] of the gold substrate (1.4 nm) was determined in air using contact mode AFM performed on a Digital Instruments Multimode Nanoscope IIIa (Santa Barbara, CA). Gold substrates were cleaned in piranha solution (70% H₂SO₄, 30% H₂O₂) for 1 min, rinsed with distilled water then ethanol, and finally dried under nitrogen. The substrates were then immersed in an ethanolic thiol solution (2 mM) for 24 h at room temperature. The substrates were removed from solution, rinsed with ethanol, and dried under a stream of nitrogen.

Contact angle measurements of the SAMs on gold were determined by the half-angle measuring method, using a CAM-PLUS MICRO Contact Angle Meter by Tantec, Inc. (Schaumburg, IL). All contact angles reported are the averages of 10 readings made on three independently prepared SAMs. The accuracy of the measurements is ±0.8°. The thickness of the

(38) Priest, C. I.; Jacobs, K.; Ralston, J. *Langmuir* **2002**, *18*, 2438−2440.

Table 1. Summary of Experimentally Determined Monolayer Thicknesses Determined by Contact Angle and Ellipsometry Measurements of SAMs of **1**−**7**

SAM	1	2	3	4	5	6	7
contact angle ± 0.8° (lit)[a]	71° (73)	78° (79)	79° (81)	61° (64)	83°	78°	82°
ellipsometry ± 1 Å (lit)[a]	13 (14)	15 (15)	14 (14)	14 (14)	11	11	12

[a] The literature values are taken from Ulman, A. *Acc. Chem. Res.* **2001**, *34*, 855−863.

SAMs on the Au surface was estimated using a Gaertner ellipsometer (Skokie, IL) (He−Ne laser, λ = 632.8 nm, angle of incidence 70°). Three separate points on two independent samples of each type of monolayer were measured and averaged, using an assumed refractive index of 1.46. The variation in the measured SAMs thickness was ±1 Å.

MNPU Crystal Growth from Solution. The α polymorph (yellow prisms) was obtained from crystallization in ethanol at 60 °C (mp = 256−258 °C). The β polymorph (white needles) was obtained from crystallization in ethyl acetate at room temperature. Upon heating, β crystals undergo a phase transformation at ∼200 °C before converting to α and melting at 256−258 °C. The γ monohydrate form (yellow plates) is obtained by a solution-mediated dissolution−recrystallization of either α and β forms after approximately 1 week of sitting in 95% ethanol solution. Ironically, this phase transformation does not seem to occur in aqueous solution. Upon heating, γ undergoes a phase transformation at ∼90 °C before converting to α and melting at 256−258 °C. We have extensively searched for but have not been able to grow crystals of the δ form.

MNPU Crystal Growth on SAMs. Saturated solutions of MNPU in either ethanol or ethyl acetate solution were prepared in vials. All SAMs were positioned such that they leaned against the side of the vial (not laying flat on the bottom), and the vials were covered with Parafilm. Crystals grown on the functionalized surface were in the range of 0.5−3 mm and typically appeared within 5−6 days. To perform experiments at 60 °C, vials were placed in a digital dry bath (Labnet, Edison, NJ). SAM substrates were first epoxied to larger strips of mica in order to prevent the substrates from falling due to any vibrations in the dry bath. Crystal growth on SAMs was attempted under multiple solvent and temperature conditions. Crystal growth was also attempted on two types of control surfaces—bare gold substrates and alkanethiol SAMs of 1-pentanethiol (Aldrich, 98+%), 1-octanethiol (Aldrich, 98.5+%), and 1-dodecanethiol (Aldrich, 98+%).

X-ray Crystallography. A Siemens SMART Platform CCD diffractometer was used to collect single-crystal X-ray diffraction data for α-, β-, and γ-MNPU crystals grown in the presence or absence of SAM templates. Unit cells matching the known crystal structures were obtained from the collection of 20 diffraction peaks, and Miller indices were subsequently assigned to all possible crystal faces.

A full data collection and structure solution of γ-MNPU was conducted at the University of Minnesota X-ray Crystallographic Laboratory. The data collection was carried out at 173 K using Mo Kα radiation (graphite monochromator). Intensity data were corrected for absorption and decay. The structure was solved and refined based on 1506 strong reflections using Bruker SHELXTL. All non-hydrogen atoms were located with a combination of direct methods and full-matrix least-squares/difference Fourier cycles and were refined with anisotropic
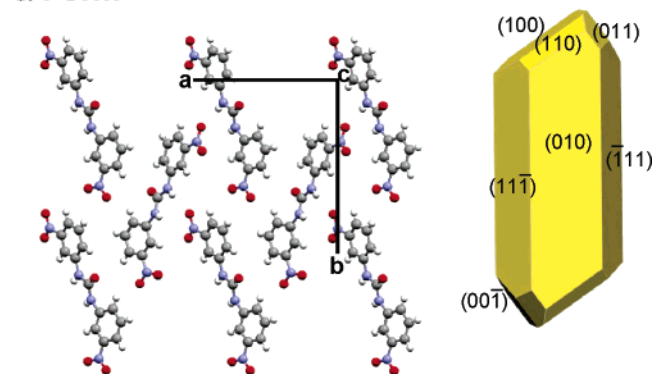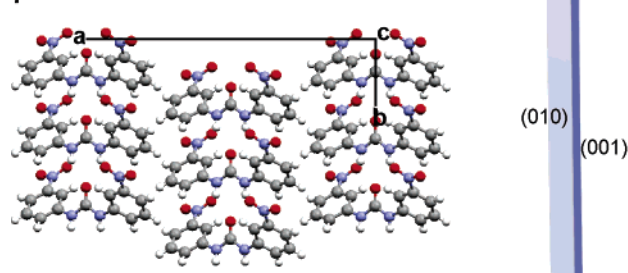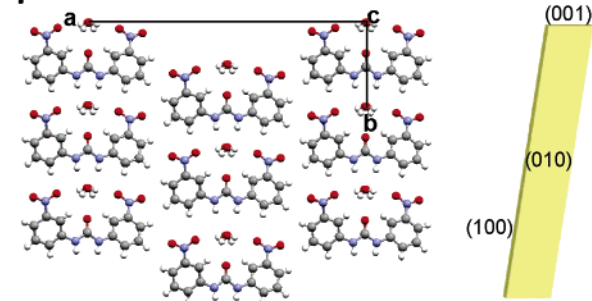
α Form

β Form

γ Form

Figure 2. Crystal packing diagrams and observed morphologies of α- (top),[35] β- (middle),[35] and γ- (bottom) MNPU constructed from fractional coordinates. Morphology figures were generated using WinXMorph, version 1.1.[39]

displacement parameters. All hydrogen atoms were placed in ideal positions and refined as riding atoms with relative isotropic displacement parameters. The final full-matrix least-squares refinement converged to $R1 = 0.0341$ and $wR2 = 0.0903$ (F^2, all data).

Results and Discussion

Molecular Conformation, Morphology, and Surface Structures of MNPU Forms. Packing diagrams of the three known forms appear in Figure 2. One of the most striking differences among the crystal structures is the conformation of the MNPU molecule. In solution, MNPU can adopt many different conformations due to the low rotational barrier about the central C−N amide bonds; however, in the solid state, the molecular conformation is fixed. In the α phase, both of the nitro groups are oriented *anti* with respect to the central carbonyl bond. In β and γ forms, both of the nitro groups are oriented *syn* with respect to the carbonyl group. In the δ form (not shown), one nitro group is *syn* to the carbonyl while the other is *anti*. These very different molecular conformations also change the in-tramolecular $O_2N\cdots NO_2$ distances between the two nitrogen

atoms. The distances are smallest in the γ monohydrate form (9.060 Å) and increase in the anhydrous β (9.937 Å), δ (11.322 Å), and α (11.629 Å) polymorphs. Readers are referred to ref 36 for additional details regarding molecular and lattice energy calculations, graph set analyses, and thermal characterizations of the various MNPU crystal forms.

For the purposes of understanding template-directed growth, our interest in these materials is focused not on their bulk structures, but rather on the topographical and chemical characteristics of the different crystal growth faces observed in the various MNPU forms. Unit cells obtained from X-ray diffraction measurements and goniometry were used to assign Miller indices to all faces of solution-grown α-, β-, and γ-MNPUs. Crystals of α and β crystals can be grown from either ethanol or ethyl acetate, and the choice of growth solvent does not appear to alter their morphologies in any significant way. α-MNPU grows as yellow prisms bounded by (010), ($\bar{1}$11), (11$\bar{1}$), (100), (110), (001), (011), and symmetry related faces (see Figure 2, top). β-MNPU grows as white needles elongated along the crystallographic *a* axis and is bounded by (100), ($\bar{1}$00), (010), (0$\bar{1}$0), (001), and (00$\bar{1}$) faces (see Figure 2, middle). γ-MNPU grows in a yellow plate-like morphology as a result of a solution-mediated transformation of either the α or β form in ethanol. Crystals of the γ form tend to grow slightly elongated in the crystallographic *c* direction and exhibit (100), ($\bar{1}$00), (010), (0$\bar{1}$0), (001), and (00$\bar{1}$) faces (see Figure 2, bottom). Previous morphological characterization of the γ form by Groth[32] suggested the presence of (110) faces, although we have not observed this. We do commonly observe higher order (*h0l*) faces in the γ form, but the exact Miller indices of these faces are hard to specify with certainty since they often appear curved. Notably, though both β and γ are polar phases, neither exhibits the polarity morphologically. All efforts to reproduce the solution growth of the δ-MNPU phase discovered by Bernstein et al. have so far been unsuccessful, although this is not the first time a particular polymorph can be grown in one laboratory and not another.[40]

Growth of MNPU on SAM Templates. In our de novo design of SAM templates that might be used to selectively nucleate individual polymorphs with high phase purity, we assumed that 2D lattice matching and/or complementary chemical matching across the SAM/crystal interface would be two critical factors. Any polymorph selectivity observed in the presence of a SAM would presumably originate from favorable interactions between the two contacting surfaces. The chemical functionality of gold−thiol monolayers is relatively easy to control with organic synthesis. For predictable control over the lattice dimensions, we regarded arenethiols to be potentially better suited to molecular crystals than the more widely used alkanethiols. Depending on the alkyl chain length, headgroup, and solvent, alkanethiols can adopt very different tilt angles with respect to the surface normal, a factor that also changes the 2D lattice periodicity on the surface. With arenethiols, close-packing considerations necessitate a more perpendicular molecular alignment at the surface. Previous studies of 4′-X-4-mercapto-biphenyl SAMs reveal that small tilt angles and herringbone packing arrangements are observed for a number of these monolayers.[37,41−43] The slightly larger size of the 2D lattice

(39) Kaminsky, W. *J. Appl. Crystallogr.* **2005**, *38*, 566−567.
(40) Dunitz, J. D.; Bernstein, J. *Acc. Chem. Res.* **1995**, *28*, 193−200.

Table 2. Crystal Growth Conditions of MNPU Relative to the Type of SAM Used, Initial Crystal Phase(s) of MNPU Used, Solvent, and Temperature

SAM	initial solute phase	solvent	temp (°C)	growth
1	α, β, or γ or any combination of phases	ethanol or ethyl acetate	25 or 60	α
2	α, β, or γ or any combination of phases	ethanol or ethyl acetate	25 or 60	β
3	α, β, γ or any combination of phases	ethanol or ethyl acetate	25 or 60	γ
4, **5**, **6**, **7**, bare gold, or alkanethiol controls	α, β, γ or any combination of phases	ethanol or ethyl acetate	25 or 60	none

dimensions afforded by aromatic SAMs (compared to alkanethiols) would also make them potentially more compatible with the typical unit cell dimensions (5−20 Å) of most molecular crystals. SAMs of 3′-X-4-mercaptobiphenyl SAMs[29] present the same types of functional groups on a 2D surface, albeit with a different orientation, and were additionally explored. Ellipsometry measurements and contact angle characterization suggest small tilt angles with respect to the normal to the gold surface, though we do not know the extent to which the general shape of these molecules might affect the long-range 2D order on the monolayer.

SAMs of **1**−**7** were introduced into saturated ethanol or ethyl acetate solutions of MNPU prepared in conventional glass vials and positioned so as to expose the gold surface to the bulk solution. To minimize the possibility of unintentional seeding due to incompletely dissolved MNPU, saturated solutions were prepared from pure α, β, or γ phases, or polymorphic mixtures. Solutions were covered with Parafilm and maintained at either room temperature (24 ± 1 °C) or at 60 °C in a digital dry bath. After sitting undisturbed for a period of 5−6 days, visible millimeter-sized crystals were consistently observed on SAMs **1**, **2**, and **3**. No MNPU crystals were ever observed on SAMs **4**−**7**. Additionally, no crystals were ever found to grow on bare gold substrates or alkanethiol monolayer (1-pentanethiol, 1-octanethiol, 1-dodecanethiol) controls.

SAMs of **1**, **2**, and **3** were each found to serve as selective nucleating templates for a single but unique MNPU phase regardless of the initial solute phase. Crystals of α-MNPU formed on monolayers of **1**, β-MNPU grew selectively on **2**, and γ-MNPU grew on **3**. Multiple crystallization experiments prepared under identical conditions confirmed the reproducibility of this effect (Table 2). The resultant crystal form obtained was completely independent of the solvent choice and/or temperature conditions explored. In all cases where growth was observed, crystals adopted preferred orientations with respect to the SAM templates, thereby illustrating the importance of the interface in the nucleation process. The three interfaces observed were SAM **1**/α-(010), SAM **2**/β-(0$\bar{1}$0), and SAM **3**/γ-(0$\bar{1}$0). We note that because the bulk and surface structures of α, β, and γ phases are different, it is sheer coincidence that the observed faces in contact with the SAMs share the same Miller indices.

(41) Sabatani, E.; Cohen-Boulakia, J.; Bruening, M.; Rubinstein, I. *Langmuir* **1993**, *9*, 2974−2981.
(42) Lee, S.; Puck, A.; Graupe, M.; Colorado, R.; Shon, Y.-S.; Lee, T. R.; Perry, S. S. *Langmuir* **2001**, *17*, 7364−7370.
(43) Shaporenko, A.; Heister, K.; Ulman, A.; Grunze, M.; Zharnikov, M. *J. Phys. Chem. B* **2005**, *109*, 4096−4103.
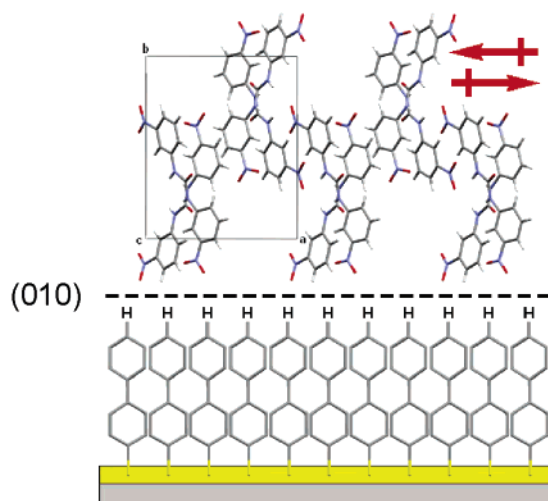
Figure 3. Selective nucleation and growth of α-MNPU on a 4-mercaptobiphenyl SAM template, SAM **1**. Top: Micrograph of an α-MNPU prism attached to SAM **1**. View is down the *b* axis. Scale bar = 0.1 mm. Bottom: Schematic of the α-(010)/SAM **1** interface. Red arrows indicate the direction of the molecular dipole moment.
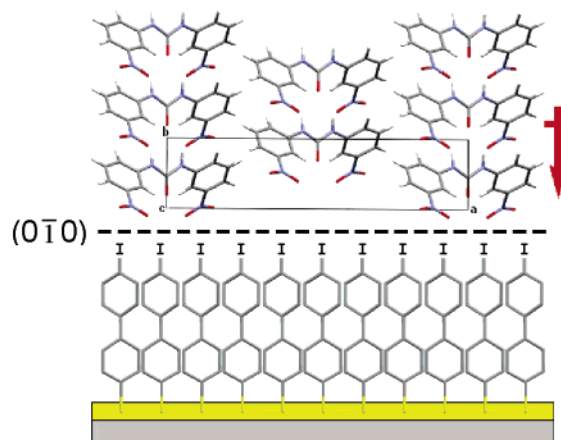

Figure 4. Selective nucleation and growth of β-MNPU on a 4′-iodo-4-mercaptobiphenyl SAM template, SAM **2**. Top: Micrograph of a β-MNPU needle attached to SAM **2**. View is down the *b* axis. Scale bar = 0.3 mm. Bottom: Schematic of the β-(0$\bar{1}$0)/SAM **2** interface. The red arrow indicates the direction of the molecular dipole moment.

Rationalizing Polymorph Selectivity. To discern the origin of the selectivity of each SAM template for a particular phase,
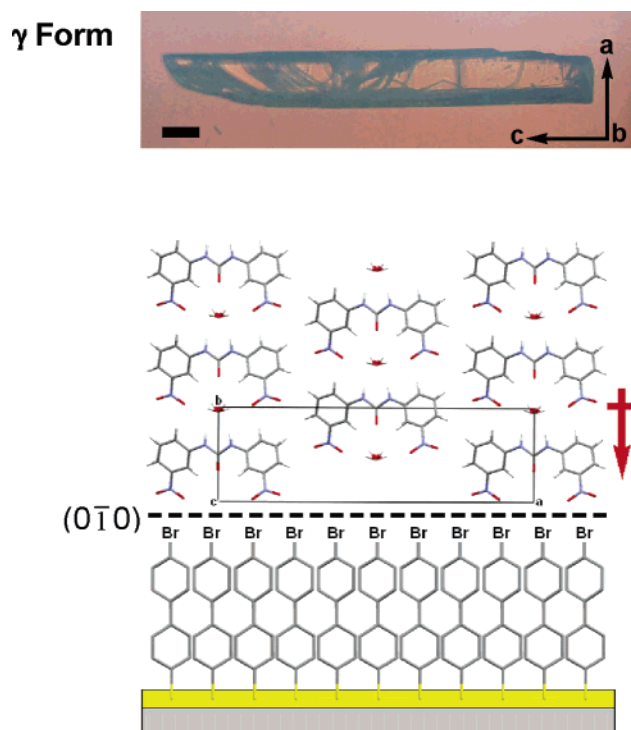
γ Form

Figure 5. Selective nucleation and growth of γ-MNPU on a 4′-bromo-4-mercaptobiphenyl SAM template, SAM **3**. Top: Micrograph of a γ-MNPU needle attached to SAM **3**. View is down the *b* axis. Scale bar = 0.3 mm. Bottom: Schematic of the γ-(0$\bar{1}$0)/SAM **3** interface. The red arrow indicates the direction of the molecular dipole moment.

each of the natural surfaces of α, β, and γ polymorphs was analyzed in terms of its specific 2D lattice dimensions and functional group orientations and densities. Molecular models of each crystal surface were constructed using Mercury 1.3 software and the relevant cif file. Such models make the intrinsic assumption that no gross surface reconstructions occur in solution and that the surface structures are nearly identical to that of the bulk plane. Some of the significant structural parameters for each observed crystal surface are provided in Table 3.

The geometric lattice matching program EpiCalc[44] was used to determine which of the crystal surfaces of the various polymorphs are epitaxially matched with the SAM. While the long-range two-dimensional molecular ordering on a single crystal surface is likely to be higher than that on a self-assembled monolayer, SAMs of 4′-X-mercaptobiphenyls are expected to exhibit domains with a high degree of 2D order.[37,43] Other authors[45,46] have previously reported the two-dimensional lattice parameters for 4′-methyl-4-mercaptobiphenyl and 4′-chloro-4-mercaptobiphenyl monolayers as 4.8 × 10.0 Å, α = 90° and 5.5 × 8.0 Å, α = 90°, respectively. On the basis of the trends observed in the SAMs characterization data (Table 1), parameters for all of the SAM surfaces used in this study are expected to have dimensions in approximately the same range. Computational screening for epitaxial relationships between all MNPU faces and the cited 4′-methyl-4-mercaptobiphenyl SAMs parameters resulted in five potential coincident matches: α-(010),

α-($\bar{1}$11), α-(11$\bar{1}$), β-(010), and γ-(001). Epitaxy screening against the 4′-chloro-4-mercaptobiphenyl parameters yielded five potential coincident matches: α-(010), α-(100), β-(010), γ-(001), and γ-(010). We note that epitaxy calculations do not distinguish between the same family of crystal faces, some of which in β and γ phases are chemically distinct. Notice that all three of the experimentally observed contacting surfaces (α-(010), β-(0$\bar{1}$0), and γ-(0$\bar{1}$0)) appear in the list, though it is not possible to predict the single best experimental match based on geometric considerations alone.

Analysis of the functional group densities on the different surfaces provides additional insight into the nature of the SAMs' templating effect. Although the strength of a single nitro···halogen interaction is small (~5.7 kJ mol⁻¹),[47,48] short NO₂···halogen contacts are frequently observed in aromatics bearing these substituents. Such interactions at SAM/crystal interfaces have also been exploited to control the orientation and polar growth direction of molecular crystals.[28] SAMs of **2** and **3** were observed to be in contact with β-(0$\bar{1}$0) and γ-(0$\bar{1}$0), respectively. Importantly, both of these MNPU phases are polar. The polar axis in each of these crystals parallels the crystallographic *b* axis. Consequently, the ±*b* faces expose different functionalities, with only the (0$\bar{1}$0) faces presenting NO₂ groups on the surface. Of all the potential surfaces listed in Table 3, the β-(0$\bar{1}$0) and γ-(0$\bar{1}$0) faces express some of the highest NO₂ densities. While the NO₂ density of γ-(100) is marginally higher than that of β-(0$\bar{1}$0), making it a potential theoretical match, the nearly parallel (4.3°) orientation of nitro groups on this surface presumably limits its ability to coordinate strongly with the halogens on the underlying substrate. Similar reasoning might also be used to discount a hypothetical preference for nucleation on the β-(100) face, in which nitro groups are high in density but oriented slightly toward the interior of the crystal and not outward on the crystal surface.

While there are a number of general similarities between the β-(0$\bar{1}$0) and γ-(0$\bar{1}$0) surfaces, recall that the molecular conformation in these phases is different. The intramolecular O₂N···NO₂ distance between nitro groups in a given molecule in the β polymorph conformation is greater than that in γ (9.937 vs 9.060 Å). It is possible that the expanded O₂N···NO₂ distance in β is slightly better suited to coordinating the larger iodine atom (*r* = 2.15 Å).[49] Coordination of the smaller bromine atom (*r* = 1.95 Å) might be preferred when the molecular conformation is more compact such as in γ. The contact angle measurements of SAMs **2** and **3** are nearly identical, so it is unlikely that SAM **3** would have a higher affinity for preexisting water which might encourage growth of the hydrated NMPU phase.

Explaining the preference for the observed α-(010) growth on the nonpolar surface of SAM **1** is more difficult. We originally hypothesized that the MNPU phase most likely to nucleate on this surface would be that which possesses the lowest NO₂ density. If this were the case, SAMs of **1** would have theoretically preferred β-(100), β-(010), or γ-(001) surfaces, which do not present any NO₂ groups on the surface. All but two of the remaining surfaces have a lower NO₂ group

(44) Hillier, A.; Ward, M. D. *Phys. Rev. B* **1996**, *54*, 14037−14051.
(45) Azzam, W.; Fuxen, C.; Birkner, A.; Rong, H.-T.; Buck, M.; Woll, C. *Langmuir* **2003**, *19*, 4958−4968.
(46) Kang, J. F.; Ulman, A.; Liao, S.; Jordan, R.; Yang, G.; Liu, G. *Langmuir* **2001**, *17*, 95−106.

(47) Hulliger, J.; Langley, P. J. *Chem. Commun.* **1998**, 2557−2558.
(48) Allen, F. H.; Lommerse, J. P. M.; Hoy, V. J.; Howard, J. A. K.; Desiraju, G. R. *Acta Crystallogr.* **1997**, *B53*, 1006−1016.
(49) Pauling, L. *The Nature of the Chemical Bond and the Structure of Molecules and Crystals—An Introduction to Modern Structural Chemistry*, 2nd ed.; Oxford University Press: London, 1940.

Table 3. Select Parameters for α-, β-, and γ-MNPU Crystal Surfaces[a]

surface	cell parameters	orientation of C–NO$_2$ bond wrt surface (0° = ∥, 90° = ⊥)	no. of unique NO$_2$ groups projecting from surface (NO$_2$ density)
α-MNPU			
(100) or ($\bar{1}$00)	8.31 × 13.82, 90°	38.7°	2 (1 per 57.42 Å^2)[b]
(010) or (0$\bar{1}$0)	8.31 × 11.50, 91.92°	20.8° (#1); 70.7° (#2)	2 (1 per 47.75 Å^2)
(001) or (00$\bar{1}$)	11.50 × 13.82, 90°	41.6° (#1); 18.4° (#2)	2 (1 per 79.46 Å^2)
(110) or ($\bar{1}\bar{1}$0)	11.50 × 13.82, 129.76°	45.2°, 23.2° (#1); 54.3°, −14.9° (#2)	3 (1 per 40.72 Å^2)
(011) or (0$\bar{1}\bar{1}$)	8.31 × 16.12, 121.01°	70.5°, −19.3° (#1); 39.8°, 22.7° (#2)	3 (1 per 38.27 Å^2)
($\bar{1}$11) or (1$\bar{1}\bar{1}$)	13.95 × 16.12, 107.01°	42.1°, 44.0° (#1); 80.6°, −8.0° (#2)	3 (1 per 71.67 Å^2)
(11$\bar{1}$) or ($\bar{1}\bar{1}$1)	13.95 × 16.12, 107.01°	44.1°, 42.2° (#1); 80.6°, −7.8° (#2)	3 (1 per 71.67 Å^2)
β-MNPU			
(100) or ($\bar{1}$00)	4.71 × 6.72, 90°	−11.9 °	0
(0$\bar{1}$0)	6.72 × 20.95, 104.96°	43.3°	4 (1 per 34.00 Å^2)[c]
(001) or (00$\bar{1}$)	4.71 × 20.95, 90°	46.5°	2 (1 per 49.34 Å^2)
γ-MNPU			
(100) or ($\bar{1}$00)	3.77 × 7.39, 90°	4.3°	1 (1 per 27.86 Å^2)
(0$\bar{1}$0)	3.77 × 24.88, 96.85°	66.1°	4 (1 per 23.28 Å^2)[d]
(001) or (00$\bar{1}$)	7.39 × 24.88, 90°	23.7°	2 (1 per 91.93 Å^2)

[a] Two-dimensional lattice dimensions are derived from fractional coordinates. The orientation of the C–N(NO$_2$) bond with respect to the surface is reported for each independent type of nitro group. NO$_2$ densities are based on the number of NO$_2$ groups presented on the outermost surface per unit cell area. [b] The (200) plane of α-MNPU exposes no NO$_2$ groups. [c] Only the (0$\bar{1}$0) face of β-MNPU presents NO$_2$ groups, none are projected on (010). [d] Only the (0$\bar{1}$0) face of γ-MNPU presents NO$_2$ groups, none are projected on (010).

density, so based on this criteria, the observed contact with the α-(010) surface seems an unlikely choice. With no obvious reason for the nucleation preference, we offer two potential hypotheses. MNPU molecules in the α form adopt an *anti−anti* conformation. The dipole moment of any one molecule is oriented nearly parallel to the C=O bond direction, but the crystal lacks a net dipole due to centrosymmetry. The molecular dipoles in α-MNPU crystals lie nearly parallel to the (010) plane. This may be the least unfavorable orientation for a highly polarized molecule to align against a relatively nonpolar surface. Given that the α-(010) surface is also the most highly corrugated, it may be more energetically favorable to undergo a surface reconstruction to a structure that is more compact. However, with the experimental methods currently available for characterizing 2D interfaces in solution, it is difficult to probe this further with sufficient molecular-level detail.

Conclusions

This study establishes that by exploiting chemical and geometric interactions at 2D self-assembled monolayer interfaces bearing different functionalities it is possible to direct the nucleation and growth of a single crystalline phase in what is otherwise a concomitant polymorphic system. Three different crystal phases of MNPU, which grow concomitantly in various combinations from solution, could each be selectively resolved with high phase purity on gold−thiol SAM templates composed of different 4′-X-4-mercaptobiphenyls. All MNPU polymorphs grown on these different SAMs adopt specific crystal orientations, which reflect their preferred geometry at the nucleation stage. The α-MNPU form grows on SAM **1**, the β-MNPU form on SAM **2**, and the γ-MNPU form on SAM **3**. The observed orientations have been rationalized on the basis of two-dimensional lattice matching (epitaxy), complementary functional group interactions, and/or dipole moments across the SAM/crystal interface. We believe this template-based strategy used to control heterogeneous nucleation events is sufficiently general and may be a useful means to direct the course of crystallization in other polymorphic systems.

Supporting Information Available: The cif file for the γ-MNPU structure has been deposited in the Cambridge Crystallographic Database. This material is available free of charge via the Internet at http://pubs.acs.org.

JA0565119